AN ANALOG ADAPTIVE BEAMFORMING CIRCUIT FOR AUDIO NOISE REDUCTION

Jeff Dugger[†] *Paul D. Smith*[⋆] *Matt Kucic*[⋆] *Paul Hasler*[†]

[†] School of Electrical and Computer Engineering
Georgia Institute of Technology
Atlanta, GA 30332

[⋆] Texas Instruments, Inc.
Santa Clara, CA

ABSTRACT

We have designed and built the first commercially available all-analog adaptive beamforming integrated circuit utilizing a dual microphone array. Beamforming performs spatial filtering by exploiting time-of-arrival differences between microphones. Our analog implementation has the advantage of using very little power which is important in portable, battery-powered devices. Rather than optimize parameters for a single filter as in a standard adaptive FIR filter used in conventional beamformers, our implementation selects among multiple filters each pre-programmed to provide various different spatial-filter patterns.

1. MULTI-MICROPHONE NOISE REDUCTION IN ANALOG VLSI

The popularity and ubiquity of cell phones and bluetooth headsets in recent years has been driving the demand for sophisticated, low-power audio noise reduction. Various approaches to this problem include both single-microphone and multi-microphone solutions. Single-microphone solutions typically utilize spectral subtraction [1]. Several multi-microphone approaches exist including beamforming [2], blind-source separation [3], and computational auditory scene analysis [4].

Of the various multi-microphone approaches, beamforming is the simplest. Beamforming performs spatial filtering by exploiting time-of-arrival differences between microphones in an array. Spatial filters provide directional patterns of attenuation where one can direct nulls for maximum attenuation in a specific direction or to provide optimal attenuation for diffuse noise fields. Adaptive filters can be used to control the directional patterns in changing noisy environments.

We have designed and built the first commercially available all-analog adaptive beamforming integrated circuit [5], which selects among multiple filters each pre-programmed for particular spatial patterns rather than adapting a single FIR filter as in standard beamformer algorithms. Our analog smart-mic array uses very little power, drawing only $210\mu A$, providing a drop-in replacement for standard electret microphones while delivering up to 30 dB of noise reduction [6].

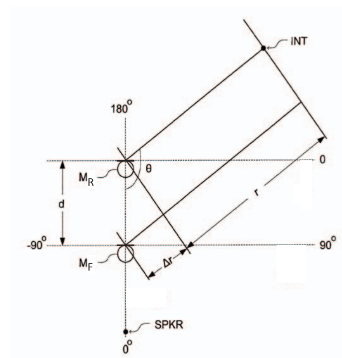

(a)

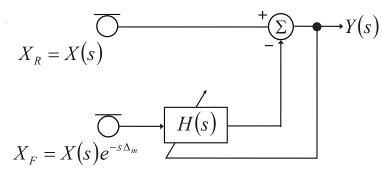

(b)

Fig. 1. *(a) Geometry of a two microphone array with desired talker and unwanted intereferer. Our derivation assumes a simple time-delay model for far-field sound wave propagation. All angles are referenced counterclockwise from the speaker. Endfire refers to directions along the axis defined by the microphone pair, while broadside refers to directions perpendicular to the endfire axis. (b) Delay-and-Sum beamformer — this simplest possible beamformer system illustrates the basic beamforming approach.*

2. ADAPTIVE BEAMFORMING NOISE CANCELLATION

Because sound signals from a desired speaker and unwanted interferers typically arise from different locations relative to the microphone, the spatial separation between the speaker and interferers can be exploited to separate the desired sound signal from the unwanted interferer using spatial filters based on beamforming [2]. Beamformer design assumes that propagation of the sound waves from each source can be adequately represented by simple time delays. Any environmental effects such as reflections, diffusion or diffraction, as well as

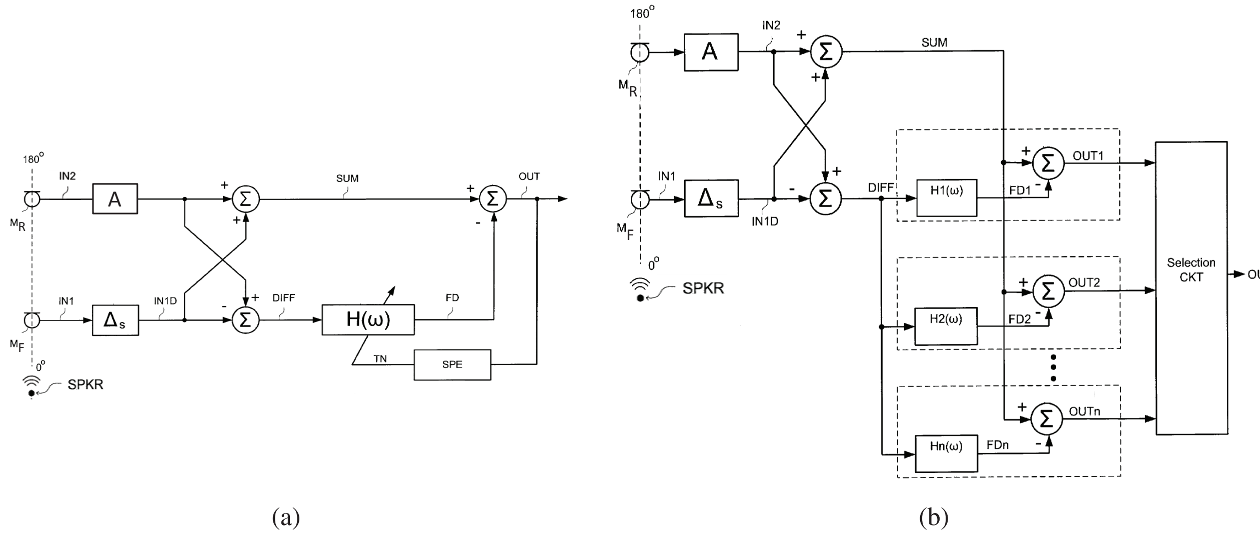

Fig. 2. *(a) Griffiths-Jim beamformer block diagram (b) Response-Select beamformer block diagram*

any effects due to mismatch of microphone spectral characteristics, will cause frequency-dependent deviations from these assumptions which can degrade the attenuation performance of the system. However, the system can still provide good, if not perfect, noise cancellation.

Figure 1 defines the geometry of the two-microphone null-steering problem. The front microphone, M_F, lies closest to the talker and we choose the back microphone, M_R, to serves as an un-delayed reference signal. Given the frequency-domain representation of a sound source as $X(s)$, equations (1) and (2) represent the signals captured by the front and back microphones respectively as

$$X_F = e^{-s\Delta_m} X(s) \tag{1}$$

and

$$X_R = X(s) \tag{2}$$

where $s = j\omega$. Referring to Fig. 1(a), we see that equation (1) defines the relative time delay between wave fronts arriving at each microphone from the far-field source as $\Delta_m = -\frac{d}{c}\cos\theta_m$, where d is the separation between the microphones, c is the speed of sound, and θ_m is the direction of arrival of the interfering source. This derivation assumes the distance from the interfering source to the microphone pair is much greater than the distance separating the two microphones. This far-field assumption simplifies the relative time delay relationship between microphones by assuming sound propagation by planar rather than spherical wave fronts and implies that the amplitudes of the signals received by both microphones are the same.

Figure 1(b) shows the simplest possible adaptive two-microphone null-steering architecture. Given a spatially localized interferer, the most straightforward method for canceling the interferer is to apply a simple adjustable delay, Δ_m , implemented by a filter $H(s)$ to X_F and subtract the resulting signal from X_R such that $Y = 0$. Automatic tuning of the null for different source directions adjusts the filter coefficients of $H(s)$, to minimize the power of the output signal, Y. Simple automatic tuning causes problems if the talker dominates the interferers in the microphone input signals, because the system will attempt to cancel the talker rather than the interferers.

Griffiths and Jim proposed a simple modification to the basic adaptive null-steering architecture (illustrated in Fig. 2(a)) that allows the system to automatically tune nulls without cancelling the talker [7]. Essentially, a fixed beam-steerer acts as a pre-processor that provides a fixed null to cancel the talker input to the adaptive filter — thus no signal due to the talker can cancel itself in the final subtraction nor can it have any impact on filter adaptation.

To create the fixed null needed to cancel the talker from the adaptive filter path, the pre-processor must ensure the input signals to the difference operation are time-aligned and their amplitudes are equal. Assuming the talker location is fixed in the endfire direction closest to the front microphone, the proper delay to time-align the inputs of the difference operation is given by $\Delta_s = \frac{d}{c}$. Although the following derivations utilize an ideal delay, Δ_s, in our analog implementation the delay is actually implemented with a second-order Bessel filter.

Because the talker usually lies in the near-field of the microphones, the talker signal amplitude on both microphones must be balanced to guarantee cancellation of the talker from the difference path. A gain term in the back microphone path given by $A = 1 + \frac{d}{r}$ provides the desired balance where it is assumed that the signal decays inversely with distance and the talker lies in the endfire direction closest to the front microphone.

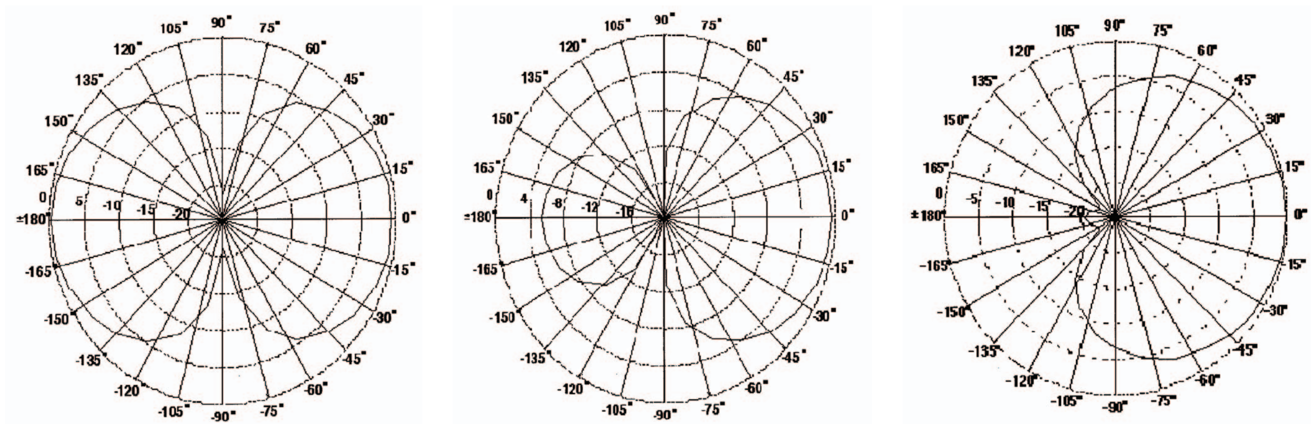

(a) (b) (c)

Fig. 3. *(a) Broadside null polar pattern (b) Hypercardioid polar pattern with null at* 109° *(c) Endfire null polar pattern*

3. RESPONSE-SELECT BEAMFORMING WITH ANALOG FILTERS

As discussed previously, automatic null-steering systems typically utilize adaptive filters. Prior research explores analog implementations of adaptive filter structures such as tapped-delay-lines and adaptive weights [8, 9, 10], but our design utilizes a novel response-select architecture [5] that avoids the complexity of implementing adaptive algorithms in silicon. The response-select architecture chooses the optimal filter output signal from among a bank of fixed filters that are pre-programmed to correspond to given directions in space relative to the microphone array. Figure 2(b) illustrates the general response-select architecture for N nulls.

3.1. Ideal Null-Filter Frequency Response

Assuming no talker signal is present, creating a null in a given direction, θ_m, requires the corresponding null block to yield $Y_m = 0$. Referring to Fig. 2(b), we see each null filter has a sum path and a difference path similar to that in the Griffiths-Jim architecture and that the output is given by

$$Y_m(s) = X_S(s) - H_m(s)\, X_D(s) = 0 \qquad (3)$$

From the response-select block diagram, observe that

$$X_S(s) = A + e^{-s\Delta'_m} \qquad (4)$$

yields the sum path signal, and

$$X_D(s) = A - e^{-s\Delta'_m} \qquad (5)$$

yields the difference path signal, where

$$\Delta'_m = \Delta_m + \Delta_s \qquad (6)$$

denotes the total delay from signal propagation and the delay filter in the Griffiths-Jim pre-processor. Substituting (4) and (5) into (3) leads to the following null-filter transfer function required to cancel an interferer from a given direction

$$H_m(s) = \frac{A + e^{-s\Delta'_m}}{A - e^{-s\Delta'_m}} \qquad (7)$$

This is the ideal transfer function to provide perfect cancellation for a localized broadband source arriving from θ_m. Unfortunately, this frequency response cannot be directly implemented as an analog filter.

3.2. Analog Approximation

Implementing the desired frequency response using a linear time-invariant analog filter requires we express (7) as a rational approximation in s with the constraint that this rational function yields a stable filter. We approximate (7) using the bilinear transform — a special case of the Padé approximant — given by

$$e^{-s\Delta'_m} \approx \frac{2-s\Delta'_m}{2+s\Delta'_m} \qquad (8)$$

Substituting (8) into (7) results in

$$H_m(s) = K\frac{s+\omega_{zm}}{s+\omega_{pm}} \qquad (9)$$

where $K = \frac{A-1}{A+1}$ provides the filter gain, $\omega_{zm} = \frac{1}{K}\frac{2}{\Delta'_m}$ yields the filter zero, and $\omega_{pm} = K\frac{2}{\Delta'_m}$ defines the filter pole. Obviously the pole of (9) lies in the left half of the s-plane, therefore (9) is a stable, continuous-time filter approximation to (7).

Our response-select beamformer adapts to changing noise and environmental conditions by selecting among the outputs of the several null-filters whose design was previously outlined. Several circuit methods could be utilized, but our implementation comprises peak-detector circuits to estimate the signal energy from each null-filter and then selects among them using hysteretic comparators.

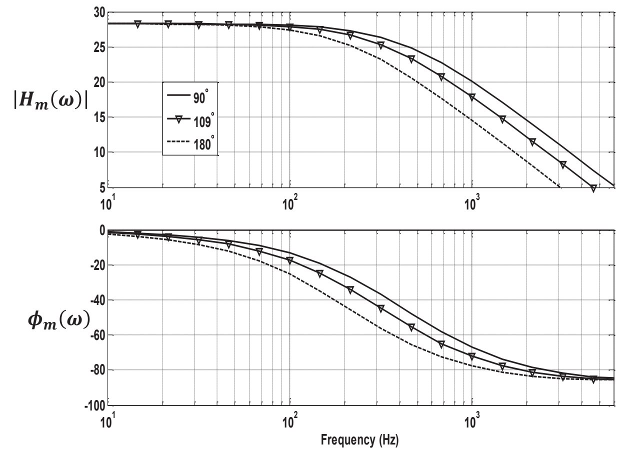

Fig. 4. *Illustration of three null-filters tuned to give the three polar patterns appearing in Fig. 3. Because the approximation in* (9) *diverges from the ideal response in* (7) *at higher frequencies, we expect the patterns to also diverge from ideal as seen in Fig. 3(c)*

3.3. Response-Select Results

We show the results of our response-select beamformer in terms of polar plots of beam patterns for three different nulls at broadside, $109°$, and endfire in Fig. 3 and the corresponding null filters in Fig. 4. The polar response patterns of Fig. 3 are composite plots generated using the root-mean-square (RMS) value of attenuation referenced to twice the signal level of the M_F input signal (which provides the 0 dB reference) over a frequency from 1 to 4 kHz. The magnitude and phase response plots in Fig. 4 show the set of null filters configured as first-order low pass filters (LPF) with corner frequencies of 521 Hz, 393 Hz, and 261 Hz corresponding to the figure-8 type polar response with nulls at $90°$ and $-90°$ shown in Fig. 3(a), a hyper-cardioid type polar response with nulls at $109°$ and $-109°$ shown in Fig. 3(b), and a cardioid type polar response with a null at $180°$ as shown in Fig. 3(c).

Referring to Fig. 3(c), note that the null at $180°$ is actually a minor lobe with symmetrical nulls near the $180°$ axis direction — this is due to deviation of the analog filter approximation from the ideal filter response. At lower frequencies, the polar response pattern of the endfire null-filter includes a null at $180°$, and the null begins to drift away from the $180°$ axis as frequency increases.

4. CONCLUSION

Unlike prior beamforming implementations, the response-select beamformer does not require an adaptive filter to continuously track changing locations of unwanted interferers. Additionally, the response-select beamformer is implemented using standard analog designs, leading to tremendous power savings over digital designs which we have shown by constructing a fully analog IC implementation that draws less than $210\mu A$ — a power drain comparable to an electret microphone alone — while providing up to 30 dB of noise rejection. The power savings of our multi-microphone analog noise reduction circuit are ideal for portable, battery-powered applications such as bluetooth headsets. It is conceivable that the design philosophy outlined in this paper could be applied to other algorithms with similar results.

5. REFERENCES

[1] Philipos C. Loizou, *Speech Enhancement: Theory and Practice*, CRC Press, 2007.

[2] B.D. Van Veen and K.M. Buckley, "Beamforming: a versatile approach to spatial filtering," *ASSP Magazine, IEEE*, vol. 5, no. 2, pp. 4 –24, april 1988.

[3] Erik M. Visser, Manabu Otsuka, and Te won Lee, "A spatio-temporal speech enhancement scheme for robust speech recognition in noisy environments," *Speech Communication*, vol. 41, pp. 393–407, 2003.

[4] H.G. Okuno and K. Nakadai, "Computational auditory scene analysis and its application to robot audition," in *Hands-Free Speech Communication and Microphone Arrays, 2008. HSCMA 2008*, may 2008, pp. 124 –127.

[5] Jeffery D. Dugger, Paul D. Smith, Paul E. Hasler, and Hans W. Klein, "Response-select null steering circuit," *U.S. Patent Application 11 / 737,127*, April 2007.

[6] National Semiconductor, Inc., "Processor for dual microphone adaptive noise cancelling with wind noise alert," *LMV1051 Product Brief*, September 2010.

[7] L. Griffiths and C. Jim, "An alternative approach to linearly constrained adaptive beamforming," *Antennas and Propagation, IEEE Transactions on*, vol. 30, no. 1, pp. 27 – 34, January 1982.

[8] Jui-Kuo Juan, J.G. Harris, and J.C. Principe, "Analog VLSI implementations of continuous-time memory structures," in *Circuits and Systems, 1996. ISCAS '96., Connecting the World., 1996 IEEE International Symposium on*, May 1996, vol. 3, pp. 338 –340 vol.3.

[9] Paul Hasler and Jeff Dugger, "Correlation learning rule in floating-gate pFET synapses," *IEEE Transactions on Circuits and Systems II*, vol. 48, no. 1, pp. 65–73, January 2001.

[10] Jeff Dugger, *Adaptive Analog VLSI Signal Processing and Neural Networks*, Ph.D. thesis, Georgia Institute of Technology, November 2003.